Eur. J. Mech. B/Fluids

WAVE GROWTH BY NON-SEPARATED SHELTERING

S.E. Belcher[1]

[1]: *Department of Meteorology, University of Reading, Reading RG6 6BB, U.K.*

(Received 5 October 1998, revised and accepted 4 January 1999)

Abstract – Atmospheric boundary layer flow over surface water waves of small slope is analysed with a new heuristic method that clearly shows the underlying physical mechanisms. In this method we consider how the wave displaces mean streamlines in the air flow. Turbulence in the air flow is found to affect the flow over the wave only in a thin inner region that lies close to the interface. The streamline displacement at the top of this inner region has three contributions: displacement over the undulating wave surface; a Bernoulli contribution associated with pressure variations over the wave (which is associated with higher wind speeds at the waves crests and lower wind speeds in the troughs); and a displacement caused by the turbulent stresses in the air flow. The displacement caused by turbulent stresses is a factor $(u_*/U_i)^2$ smaller than the other two contributions (u_* is the friction velocity and U_i is the wind speed at the top of the inner region), but is important because it leads to the winds being slightly faster on the upwind side of the wave crest compared to in the lee and to the streamline-displacement pattern being shifted slightly downwind of the wave crest. This then leads to a small surface pressure difference across the wave crest and thence wave growth. This is the *non-separated sheltering mechanism.* The solutions obtained here using physically-based heuristic arguments are in full agreement with those calculated using formal asymptotic methods by Belcher & Hunt (1993) and Cohen & Belcher (1999). The understanding gained from the new method suggests a nonlinear correction to the formula for wave growth that tends to reduce the wave growth rate for steeper waves, in agreement with computations.

1. Introduction

Jeffreys (1925) put forward the *sheltering mechanism* of wind-induced growth of surface water waves, whereby the air flow is assumed to separate in the lee of the wave crest leading to a pressure difference across the wave crests, which Jeffreys showed leads to wave growth. Hence Jeffreys found the wave growth rate in terms of an undetermined parameter, which he called the sheltering coefficient.

More recently, understanding developed in studying atmospheric boundary layer flow over hills (e.g. Hunt, Leibovich & Richards 1988; Belcher, Newley & Hunt 1993) has been used to further our understanding of boundary layer flow over waves, and in particular their wind-induced growth. Most ocean waves have gentle slopes and separation does not occur, and the recent studies show how for these gentle waves turbulent stresses in the air flow lead to a reduction in wind speed in the lee, so that streamlines reach their maximum vertical displacement slightly downwind of the wave crest (see figure 1). There is then an associated pressure difference across the wave and so also wave growth. Hence over waves of small slope, and no separation, there is a *non-separated sheltering* that leads to growth of the waves (Belcher & Hunt 1993; Miles 1993, 1996; van Duin 1996b; Zou 1998). This mechanism, which is associated with turbulence in the wind, complements the celebrated *critical-layer mechanism* of wave growth first analysed by Miles (1957), which is an inviscid shear-flow instability. There have been studies of how the non-separated sheltering and the critical-layer mechanisms act together (Miles 1993, 1996; Belcher, Hunt & Cohen 1998), but no definitive conclusions have been reached. These developments have been reviewed recently by Belcher & Hunt (1998).

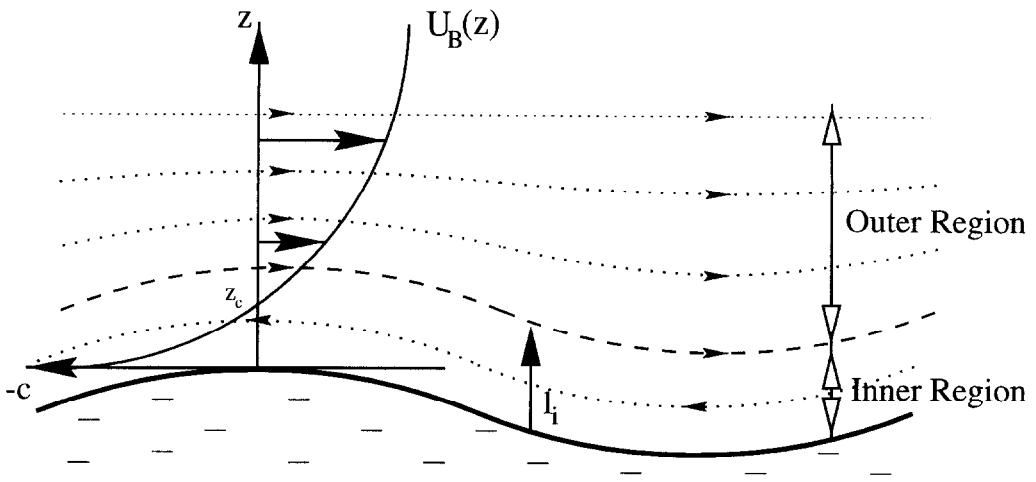

FIGURE 1. Schematic of the flow geometry. Notice how there is sheltering in the lee, with the maximum displacement of the streamline slightly downwind of the wave crest

The detailed and rigorous analyses of non-separated sheltering over slow waves (Belcher & Hunt 1993) and fast waves (Cohen & Belcher 1999) is mathematically involved. The purpose of this paper, therefore, is to develop a more heuristic method, with no intention of rigour, but which sheds light on the physical processes responsible for non-separated sheltering. The present method is based on analysing the displacement of streamlines over the wave and is based on the elegant formalism introduced by Miles (1993). Belcher, Hunt & Cohen (1998) have recently shown how the critical-layer mechanism of wave growth can be understood within a similar framework. Hence the present study represents a step towards analysing together the effects of non-separated sheltering and the critical layer. Finally, a general advantage of more heuristic methods is that they distinguish the key physical assumptions from the mathematical assumptions and so can help to show how the results can be extended to more general situations, and here the new analysis suggests how the results can be generalised for waves of moderate slope, when nonlinear effects are significant.

In §2 the streamline displacement is defined and the basic linear model of the air flow is formulated. In §3 the displacement of streamlines is calculated and in particular the contribution to the streamline displacement from the turbulent stress is evaluated. The results are then used in §3.4 to determine the pressure at the wave surface and turbulent stress at the wave surface. The physical interpretation of these calculations is given in §3.5. The wave growth rate is calculated in §4. Finally in §4.2 a nonlinear correction is suggested for the growth rate formula.

2. Formulation of the physical model

Define the basic flow, which occurs in the limit of vanishing waves when the interface is flat and located at $z = 0$. In the basic flow the wind blows in the positive x-direction with a logarithmic velocity profile, namely $\overline{U}_B = (u_*/\kappa)\ln(z/z_0)$, where κ is the von Karman constant (taken here to be 0.4), and z_0 is the roughness parameter. The shear stress in this basic flow, τ_B, is constant with height and equal to u_*^2, in a normalisation where the density of the air is one (so that the density of water is ρ_w/ρ_a), and where u_* is the friction velocity. We calculate the linear changes to this basic flow caused by a two-dimensional wave of small slope that travels along the air-water interface in the wind direction. Then it is sufficient to consider sinusoidal water waves described by $z_s = \mathrm{Re}\{ae^{\mathrm{i}kx-ct}\}$, where a is the wave amplitude, k is the wavenumber, and the wave slope is $ak \ll 1$.

2.1. *Formulation in streamline coordinates*

Calculations are performed in a reference frame moving with the wave crests, when at leading order the basic wind profile is simply displaced over the wave surface and can be written

$$U_B = \frac{u_*}{\kappa} \ln\{(z-s)/z_0\} - c. \tag{2.1}$$

Here s is the vertical displacement of a mean streamline from its position in the unperturbed flow. Following Miles (1993), perturbations to the airflow induced by the travelling wave are analysed in terms of $s(\xi,\eta)$, where η is the height of the undisturbed streamlines from the undisturbed water surface. The streamfunction, ψ, is then given by $\psi = \int U_B(\eta)\mathrm{d}\eta$. The following analysis of air flow over the waves is then performed in a streamline coordinate system, (ξ,η), defined by

$$x = \xi, \quad z = \eta + s(\xi,\eta).$$

The horizontal and vertical components of the wind over the wave, u and v, written in terms of this streamline coordinate system, are

$$u = U_B + \tilde{u} = \frac{U_B(\eta)}{1+\partial s/\partial\eta} \approx U_B(1-\partial s/\partial\eta), \tag{2.2}$$

$$w = \tilde{w} = \frac{U_B(\eta)\partial s/\partial\xi}{1+\partial s/\partial\eta} \approx U_B\partial s/\partial\xi, \tag{2.3}$$

where the approximate forms are for waves of small slope. Upper case letters with subscripts B denote variables associated with the basic flow, and an overbar denotes basic-state variables measured in the laboratory frame, otherwise the reference frame moves with the wave crests. The symbols $\tilde{u}$ and $\tilde{w}$ denote the wave-induced perturbations to the horizontal and vertical velocity.

If the Reynolds-averaged momentum equations are transformed into the streamline coordinate system and then linearised for small wave-induced perturbations, then the horizontal and vertical momentum equations are

$$U_B\frac{\partial\tilde{u}}{\partial\xi} = -\frac{\partial\tilde{p}}{\partial\xi} + \frac{\partial\tilde{\tau}}{\partial\eta}, \tag{2.4}$$

$$U_B\frac{\partial\tilde{w}}{\partial\xi} = -\frac{\partial\tilde{p}}{\partial\eta} + \frac{\partial\tilde{\tau}}{\partial\xi}, \tag{2.5}$$

which show the power of the streamline coordinate system, namely that the advective rates of change are only in the ξ-direction, i.e. along the streamlines. Here, $\tilde{\tau}$ is the wave-induced turbulent shear stress; the wave-induced normal turbulent stresses are neglected in the analysis here because their effects are smaller than the dominant terms calculated (Townsend 1972).

The boundary condition on u at the wave surface is the no-slip condition, so that the wave-induced flow must match the tangential velocity associated with the orbital motions in the water, $\tilde{u}_s$. The boundary condition on w ensures that the surface is a streamline, i.e. $w(z_0) = Dz_s/Dt$. Hence

$$\tilde{u} = \tilde{u}_s, \quad \tilde{w} = -c\mathrm{d}z_s/\mathrm{d}\xi \quad \text{on } \eta = z_0. \tag{2.6}$$

This shows a second advantage of the streamline coordinates, namely that boundary conditions can be applied actually at the boundary, rather than being linearised onto a horizontal surface. In addition, the wave-induced flow decays to zero far above the air–water interface, i.e.

$$\tilde{u}, \tilde{w} \to 0 \quad \text{as} \quad k\eta \to \infty. \tag{2.7}$$

2.2. *Modelling the wave-induced turbulent stress*

As Townsend (1972) and others have argued, to model the wave-induced turbulent stress faithfully, the flow in the air needs to be divided into two regions (figure 1). In an *inner region* that lies close to the wave surface the turbulence approaches an equilibrium with the mean-flow velocity gradient and so a mixing-length model can be used. In an *outer region* the turbulence is advected over the wave too quickly for it either to adjust to the mean velocity gradient or for it to transport significant momentum vertically. The wave-induced turbulent stresses in the outer region can be calculated using rapid-distortion theory (Britter, Hunt & Richards 1981; Belcher & Hunt 1993), which shows that they are small and so can be neglected compared with the pressure gradient forces in (2.4) and (2.5). These arguments are reviewed fully in Belcher & Hunt (1998), and have been shown to be consistent with measuremrents by Mastenbroek et al. (1996).

The height dividing the inner and outer regions, $\eta = l_i$, is determined from scaling arguments by balancing the time it takes for an eddy to be advected over the wave with the time it takes for an eddy to decorrelate. This procedure leads to l_i being determined implicitly from

$$kl_i = 2\kappa u_*/|U_i|, \tag{2.8}$$

where $U_i = U_B(l_i)$, so that for a logarithmic wind profile

$$kl_i|\ln(l_i/z_0) - \kappa c/u_*| = 2\kappa^2. \tag{2.9}$$

In summary then, in the inner region $\eta < l_i$ the mixing-length model is used to describe the wave-induced stress, namely

$$\tilde{\tau}_{ml} = 2\kappa u_* \eta \partial\tilde{u}/\partial\eta. \tag{2.10}$$

and in the outer region the wave-induced stress is set to zero. A model for $\tilde{\tau}$ can be formed over the whole depth of the air flow by interpolating between the two extremes,

$$\tilde{\tau} = \tilde{\tau}_{ml} e^{-k\eta/\delta^n}, \tag{2.11}$$

where $0 < n < 1$ is a model constant, $\delta = u_*/U_1$ and $U_1 = U_B(k^{-1})$. The wave-induced stress is then forced to zero in an overlap between the inner and outer regions.

Now, as figure 2 shows, the height of the inner region, l_i, varies with the wind and wave speeds, encapsulated in the ratio c/u_*. In particular for *slow waves*, c/u_* less than about 10, and for *fast waves*, c/u_* greater than about 20, the inner region is a thin layer so that $kl_i \ll 1$. Furthermore, in these limits the critical layer does not play a dynamical role in the air flow because it is very close to the surface for slow waves (Belcher & Hunt 1993) and because it is very far from the surface for fast waves (Cohen & Belcher 1999). The growth of small-amplitude waves is then dominated by the non-separated sheltering as shown next.

3. Perturbed flow in the inner and outer regions

Here we derive the solution for the streamline displacement following a heuristic method, based on ideas originally developed by Hunt & Richards (1984) for flow over hills and extended by Belcher & Hunt (1998). The method is valid whenever the inner region is thin, and so the solutions found here apply both to slow and to fast waves. The results of the heuristic calculations developed here will be compared with the formal asymptotic solutions found for slow waves by Belcher & Hunt (1993) and for fast waves by Cohen & Belcher (1999).

3.1. *Streamline displacement in the inner region*

Consider the streamline displacement, $s(\xi, \eta)$, at the 'top' of the inner region, at $\eta = l_i$, denoted here by $s_i(\xi)$. The location of the displaced streamline is $l_i + s_i(\xi)$. To estimate the magnitude of $s_i(\xi)$ rearrange (2.2),

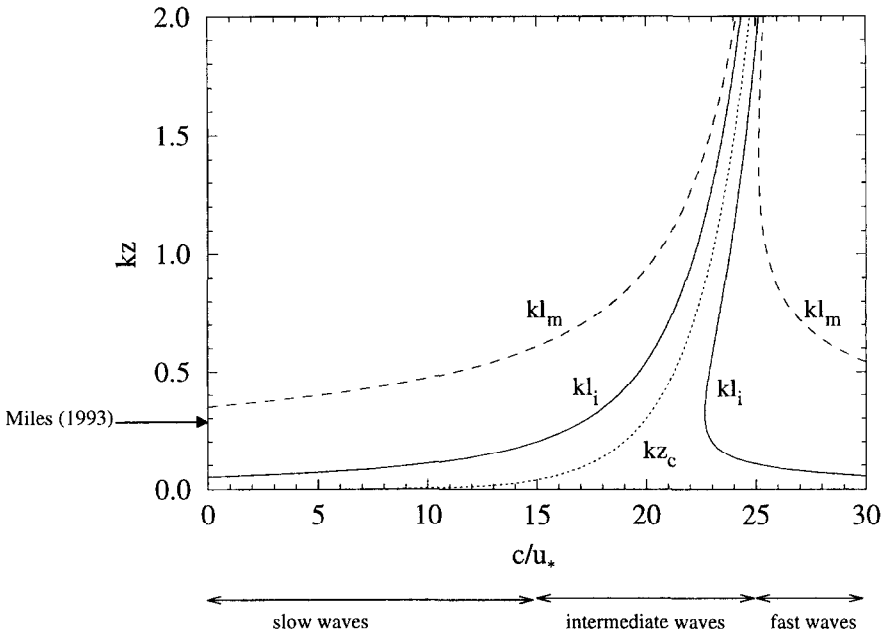

FIGURE 2. Variation with c/u_* of the inner region height (solid lines), critical height (dotted line) and middle layer height (dashed line) when $kz_0 = 10^{-4}$. The arrow shows the value for kl_m used by Miles (1993)

which relates $\tilde{u}$ and s, to give the streamline displacement in terms of the horizontal velocity perturbation

$$s_i(\xi) = z_s(\xi) - \int_{z_0}^{l_i} (\tilde{u}/U_B)\mathrm{d}\eta. \tag{3.1}$$

The first term, $z_s(\xi) = \mathrm{Re}\{ae^{ik\xi}\}$, follows from the kinematic boundary condition that the wave surface is a streamline. Equation (3.1) expresses mass conservation across the inner region: if the air speeds up, so that $\tilde{u} > 0$, then the streamline is displaced downwards.

Now, $\tilde{u}$ can be estimated using the horizontal momentum equation (2.4), together with the approximation that because the inner region is thin, $kl_i \ll 1$, the pressure there is approximately constant with height, i.e. $\tilde{p}(\xi,\eta) \approx \tilde{p}(\xi,z_0) \equiv \tilde{p}_s(\xi)$. Hence combining (3.1) with (2.4) shows that $s_i(\xi)$ can be expressed as a sum of effects:

$$s_i(\xi) \approx z_s(\xi) + l_i\frac{\tilde{p}_s(\xi)}{U_i^2} + s_\tau(\xi), \tag{3.2}$$

where, following the Oseen approximation for laminar boundary layers, $\int_{z_0}^{l_i}(1/U_B^2)\mathrm{d}\eta$ is approximated by l_i/U_i^2 to give the second term. (Corrections to this approximation are largest very near the surface, within $\eta < (l_i z_0)^{\frac{1}{2}}$, but there the streamlines follow the wave surface and so (3.2) remains a good approximation.) Equation (3.2) shows that the streamline displacement is composed of the sum of displacement by the wave itself, a Bernoulli

variation of streamline height associated with pressure variations, and a displacement caused by the change in shear stress across the inner region, which is given by

$$s_\tau(\xi) = \int^{\xi} \frac{1}{U_B^2}\{\tilde{\tau}_s(\xi) - \tilde{\tau}_i(\xi)\}\mathrm{d}\xi. \tag{3.3}$$

Hence, deceleration of the air by a change in wave-induced shear stress across the inner region, $\tilde{\tau}_s - \tilde{\tau}_i$, leads to reduced air speeds and hence upward streamline displacement.

3.2. *Evaluation of* s_τ

As explained in §2.2, the wave-induced stress is negligibly small in the outer region. Furthermore, as explained in §3.1, in the inner region the pressure is approximately constant with height. Hence in an overlap between the inner and outer regions, where both approximations apply, the momentum equation (2.4) yields

$$\tilde{u}(\xi,\eta) \approx -\tilde{p}_s(\xi)/U_B(\eta), \tag{3.4}$$

so that when $\eta \approx l_i$, $\tilde{u} \approx -\tilde{p}_s/U_i$.

Within the inner region the turbulent stresses act to reduce this streamwise velocity perturbation to satisfy the surface boundary condition (2.6). Hence the inner region acts as an internal boundary layer. To a crude approximation this leads to a logarithmic variation of $\tilde{u}$ with height from its value at the surface, $\tilde{u}_s(\xi)$ at $\eta = z_0$, up to its value at the top of the inner region, $\eta \approx l_i$. Then, if the wave-induced surface stress is $\tilde{\tau}_s$, the wave-induced velocity has the form

$$\tilde{u} \approx \frac{1}{2}\frac{(\tilde{\tau}_s/u_*)}{\kappa}\ln(\eta/z_0) + \tilde{u}_s. \tag{3.5}$$

But matching this with the solution (3.4) for $\tilde{u}$ at $\eta \approx l_i$ yields

$$\tilde{\tau}_s \approx \frac{2\kappa u_*}{\ln(l_i/z_0)}\{\tilde{u}_i - \tilde{u}_s\} \approx -\frac{2\kappa u_*}{\ln(l_i/z_0)}\{\frac{\tilde{p}_s}{U_i} + \tilde{u}_s\}. \tag{3.6}$$

The more detailed solutions (Belcher & Hunt 1993; Cohen & Belcher 1999) show how the logarithmic velocity profile near the surface joins smoothly with the inviscid solution above the inner region. However, the solution for the surface stress given in (3.6) agrees with the value obtained from the formal asymptotic analysis (Cohen & Belcher 1999 equations 5.41 and 5.42).

In addition, the wave-induced stress at $\eta \approx l_i$ is calculated from the solution (3.4) for $\tilde{u}$ to give

$$\tilde{\tau}_i = 2\kappa u_* l_i \frac{\partial \tilde{u}}{\partial \eta} = 2\kappa u_* l_i \frac{U_B'(l_i)}{U_i^2}\tilde{p}_s(\xi) = 2\frac{u_*^2}{U_i^2}\tilde{p}_s(\xi). \tag{3.7}$$

Hence it follows from (3.3), (3.6) and (3.7), that

$$\begin{aligned} s_\tau(\xi) &\approx -\frac{1}{U_i^2}\int^{\xi}\left[\left\{\frac{2\kappa u_*}{U_i\ln(l_i/z_0)} + \frac{2u_*^2}{U_i^2}\right\}\tilde{p}_s(\xi) + \frac{2\kappa u_*}{\ln(l_i/z_0)}\tilde{u}_s(\xi)\right]\mathrm{d}\xi \\ &= -\frac{1}{\mathrm{i}kU_i^2}\left[\left\{\frac{2\kappa u_*}{U_i\ln(l_i/z_0)} + \frac{2u_*^2}{U_i^2}\right\}\tilde{p}_s(\xi) + \frac{2\kappa u_*}{\ln(l_i/z_0)}\tilde{u}_s(\xi)\right], \end{aligned} \tag{3.8}$$

when $z_s = ae^{\mathrm{i}k\xi}$. This expression, which is valid both for fast and slow waves, is extremely interesting, because it shows how the frictional effect of the Reynolds shear stress in the inner region gives rise to a phase shift in the streamline displacement: the maximum in the streamline displacement is shifted a small distance (downwind for slow waves, upwind for fast waves) away from the wave crest, to $k\xi = O(u_*^2/U_i^2)$.

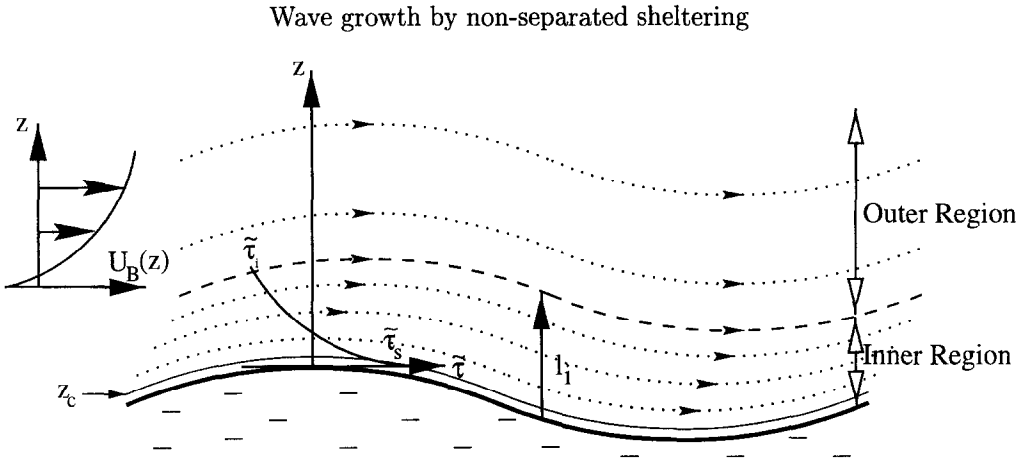

FIGURE 3. Non-separated sheltering over slow waves

3.3. *Streamline displacement in the outer region*

As explained in §2.2, in the outer region, the shear stress gradient is smaller than the pressure gradients, so that, in the outer region, (2.4) and (2.5) combine to give an inviscid equation for the streamline displacement, namely

$$U_B^2 \frac{\partial^2 s}{\partial \xi^2} + \frac{\partial}{\partial \eta}\left(U_B^2 \frac{\partial s}{\partial \eta}\right) \approx 0. \tag{3.9}$$

For a logarithmic basic flow (2.1), the basic velocity profile in this equation can be taken to be approximately constant with height (because U_B'/kU_B is small when $k\eta \approx 1$). The dynamics in the outer region (3.9) then reduces to potential flow

$$\frac{\partial^2 s}{\partial \xi^2} + \frac{\partial^2 s}{\partial \eta^2} \approx 0 \quad \text{so that } s \approx s_0\, e^{-k\eta} e^{ik\xi}, \tag{3.10}$$

The constant s_0 is determined by matching this solution with the streamline displacement at the top of the inner region, s_i, given in (3.2). Now, from (3.10), $s(\xi,\eta) \approx s_0\{1 - k\eta\}$, which matches (3.2) if

$$s_0 = z_s + s_\tau. \tag{3.11}$$

Hence, to this leading-order approximation, the streamline displacement in the outer region decays exponentially from its value at the top of the inner region: no further phase shift is generated by the shear stress in the outer region. As far as the outer region is concerned the flow is over a wave whose surface is given by $z_s + s_\tau$, which is shifted slightly downwind of the crest of the water surface (see figure 3).

3.4. *The wave-induced pressure*

The wave-induced pressure can be calculated conveniently from the vertical momentum equation (2.5) with the boundary condition that the wave-induced pressure far from the surface is zero, so that

$$p(\eta) = -\int_\eta^\infty \left\{-U_B \frac{\partial \tilde{w}}{\partial \xi} + \frac{\partial \tilde{\tau}}{\partial \xi}\right\} \mathrm{d}\eta, \tag{3.12}$$

so that we might think of the streamwise pressure gradient, $\partial \tilde{p}/\partial \xi$, driving the wave-induced flow and the vertical pressure gradient responding to the vertical structure of the resulting wave-induced flow.

We saw above in §3.3 that in the outer region the streamline displacement is determined approximately by potential flow, with solution (3.10), so that the wave-induced horizontal and vertical velocities, calculated from (2.3) and (2.2), are respectively

$$\tilde{u} = -U_B k s_0 e^{-k\eta} e^{\mathrm{i}k\xi}, \quad \tilde{w} = U_B \mathrm{i} k s_0 e^{-k\eta} e^{\mathrm{i}k\xi}, \tag{3.13}$$

and the wave-induced shear stress, calculated from (2.11) is

$$\tilde{\tau} = \{2\kappa u_* \eta \partial\tilde{u}/\partial\eta\} e^{-k\eta/\delta^n} e^{\mathrm{i}k\xi} \approx -\, 2\kappa u_* U_B\, k^2 s_0 \eta\, e^{-k\eta/\delta^n} e^{\mathrm{i}k\xi}, \tag{3.14}$$

which therefore decays to zero over the same length scale as the damped mixing-length model.

Turning back to the pressure variation itself, these solutions for $\tilde{w}$ and $\tilde{\tau}$ can be substituted into the integral (3.12), which yields

$$\tilde{p}(\xi,\eta) = -e^{\mathrm{i}k\xi} \int_\eta^\infty \left\{ U_B^2 k^2 s_0 e^{-k\eta} - 2\kappa u_* U_B\, \mathrm{i}k^3 s_0 \eta\, e^{-k\eta/\delta^n} \right\} \mathrm{d}\eta. \tag{3.15}$$

The first term in (3.15) represents the inviscid part of the wave-induced pressure and can be written $V^2 k s_0 e^{\mathrm{i}k\xi}$, where

$$V^2(k\eta) = \int_{\hat{\eta}}^\infty U_B^2 e^{-\hat{\eta}} \mathrm{d}\hat{\eta}, \tag{3.16}$$

(here $\hat{\eta} = k\eta$) is the square of a weighted average wind speed. Miles (1993) calculates the solution for $V(z_0)$ explicitly for a logarithmic basic wind profile. However a more general method can be used to estimate V for arbitrary basic wind profiles if (3.16) is integrated by parts:

$$V^2 = \left[-U_B^2 e^{-\hat{\eta}}\right]_{\hat{\eta}}^\infty + \int_{\hat{\eta}}^\infty 2(U_B U_B'/k) e^{-\hat{\eta}} \mathrm{d}\hat{\eta}, \tag{3.17}$$

Now the second term is smaller than the first term because U_B'/kU_B is small over most of the outer region. However, towards the surface this ratio increases until it is equal to one at height l_m, defined implicitly by

$$k l_m \approx |U_m'/kU_m|, \quad \text{so that} \quad k^2 l_m^2 |\ln(l_m/z_0) - \kappa c/u_*| = 1, \tag{3.18}$$

for a logarithmic basic velocity profile. The subscript 'm' is used to denote this level because l_m corresponds to the height of the middle layer defined by Hunt et al. (1988). Variation of l_m with c/u_* is shown in figure 2; also marked is the value obtained by Miles (1993). For slow and fast waves kl_m is small and so the pressure changes from $\eta = l_m$ to the surface are a factor kl_m smaller than $\tilde{p}(l_m)$. Hence $\tilde{p}_s \approx \tilde{p}(l_m)$. Furthermore, the foregoing arguments suggest that $\tilde{p}(l_m) \approx V^2(l_m) k s_0 e^{\mathrm{i}k\xi}$, and also that $V^2(l_m) \approx U_m^2$ (where $U_m = U_B(l_m)$) since $kl_m \ll 1$. Hence the inviscid contribution to the surface pressure is approximately $U_m^2 k s_0 e^{\mathrm{i}k\xi}$.

The second term in (3.15) arises from horizontal variations in the wave induced stress in the outer region and can be integrated to give a surface value of $-2\kappa u_* U_m \delta^{2n}\, \mathrm{i}k s_0$. Hence the damping of the mixing-length model leads to a small variation of pressure with height.

The pressure at the wave surface is therefore given by

$$\begin{aligned} \tilde{p}_s &\approx \left[-U_m^2 \{kz_s + ks_\tau\} + 2\kappa u_* U_m \delta^{2n} \mathrm{i}k\{z_s + s_\tau\}\right] e^{\mathrm{i}k\xi} \\ &= -U_m^2 k z_s \left\{1 - \mathrm{i}\frac{u_*^2}{U_m^2}\beta\right\} e^{\mathrm{i}k\xi}. \end{aligned} \tag{3.19}$$

Here $\beta = \beta_{z_s} + \beta_{\tilde{u}_s} + \beta_o$, which represent contributions from: the streamline displacement caused by the shear stress in the inner region, which has two components the contribution caused by the undulating wave surface,

β_{z_s}, and the contribution from the varying surface velocity, $\beta_{\tilde{u}_s}$; and the pressure variation across the outer region, which gives β_o. If products of small terms are neglected, then from (3.8) the values of these contributions are

$$\beta_{z_s} = \frac{U_m^2}{U_i^2}\left[\frac{2U_m^2}{U_i(u_*/\kappa)\ln(l_i/z_0)} + \frac{2U_m^2}{U_i^2}\right] = 2\left(\frac{\overline{U}_m - c}{\overline{U}_i - c}\right)^4\left\{2 - \frac{c}{\overline{U}_i}\right\}, \tag{3.20}$$

$$\beta_{\tilde{u}_s} = -\frac{2U_m^2}{U_i^2(u_*/\kappa)\ln(l_i/z_0)}\frac{\tilde{u}_s}{kz_s} = -2\left(\frac{\overline{U}_m - c}{\overline{U}_i - c}\right)^2\frac{c}{\overline{U}_i}, \tag{3.21}$$

$$\beta_o = \frac{2\kappa\delta^{2n}U_m}{u_*} = 2\kappa\delta^{2n}\left\{\frac{\overline{U}_m - c}{u_*}\right\}. \tag{3.22}$$

These expressions agree with the solutions found using formal asymptotic methods by Cohen & Belcher (1999), equations (5.37) and (5.38).

Results from the foregoing analysis can be used to evaluate the wave-induced shear stress at the wave surface, which is written $\tilde{\tau}_s = \mathrm{Re}\{kz_s u_*^2(\gamma + \mathrm{i}\epsilon)e^{\mathrm{i}k\xi}\}$. In the following γ only is required. There are two contributions to γ, namely from the undulating wave surface, denoted γ_{z_s}, and from the varying surface velocity, denoted $\gamma_{\tilde{u}_s}$. The result (3.6), together with the solution (3.19) for the surface pressure, show that they are given to leading order by

$$\gamma_{z_s} = \frac{2\kappa U_m^2}{U_i u_* \ln(l_i/z_0)} = \frac{2(\overline{U}_m - c)^2}{(\overline{U}_i - c)\overline{U}_i}, \quad \gamma_{\tilde{u}_s} = -\frac{2\kappa\tilde{u}_s}{u_*\ln(l_i/z_0)kz_s} = -\frac{2c}{\overline{U}_i}. \tag{3.23}$$

These results will be useful in §4 below, when the wave growth rate is calculated.

3.5. *Discussion*

The solutions derived here are valid provided the inner region is a thin layer, so that $kl_i \ll 1$. The conditions required to keep $kl_i \ll 1$ are established in Cohen & Belcher (1999) and correspond to slow waves, with $\kappa c/u_*$ of order one (so that in practice $c/u_* < 15$), and to fast waves, with c/U_1 of order one (so that in practice $c/u_* > 25$). That the same reasoning has led to results applicable to these two regimes is noteworthy. The solutions are not valid in the intermediate regime, which corresponds to wind–wave systems with $15 < c/u_* < 25$, because the inner region is no longer thin and also because the critical height is of the same order as the depth of the inner region, so that $\overline{U}_i \approx c$ and the governing equation is singular. Resolution of this singularity requires explicit analysis of the critical layer, which is beyond the scope of this paper.

The analysis shows that the streamline displacement at the top of the inner region has three contributions: a displacement by the undulating wave surface, a displacement associated with pressure variations along the streamline (which tends to be negative at the wave crest, where the pressure is lowest and the air speeds are highest) and finally a displacement, s_τ, due to the wave-induced stress change across the inner region. The solution (3.8) shows that s_τ is a factor u_*/U_1 smaller than the other two terms and so the streamline displacement at the top of the inner region is largely independent of the turbulent stress. In the outer region the wave-induced stress is negligible and so again, the streamline displacement, which towards the surface matches the value at the top of the inner region, is largely independent of the turbulent stress and to a good approximation is just exponential decay.

Although small, s_τ is important. It is related, via (3.3), to the integral along a streamline of the change in wave-induced stress across the inner region. Hence, as an air parcel moves along a streamline the frictional deceleration from the change in wave-induced turbulent stress leads to an accumulated displacement of the streamline and hence the maximum streamline displacement is downwind of the wave crest. Belcher & Hunt (1993) called this process *non-separated sheltering*. For slow waves, the basic flow in the inner region is from left to right, i.e. in the same direction as the wave propagates, and so the displacement in the streamlines is to the right of the wave crest (figure 3), but for fast waves the basic flow is from right to left, i.e. against the direction

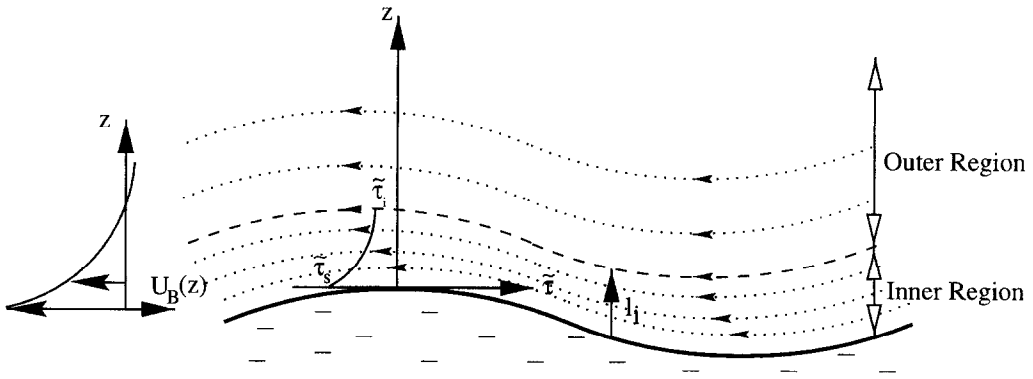

FIGURE 4. Non-separated sheltering over fast waves

of propagation, and the streamlines are also displaced slightly to the left (figure 4). This small displacement of streamlines at the top of the inner region also means that streamlines in the outer region are displaced slightly downwind of the wave crest. The pressure perturbation that develops in the outer region then has its minimum displaced downwind of the wave crest, which leads to the contribution to the surface pressure denoted by β_{z_s}. Orbital motions at the wave surface also lead to a change in wave-induced stress across the inner region that is negative and leads to a sheltering displacement of the streamline at the top of the inner region upwind of the wave crest. This process leads to a small shift in the surface pressure denoted by $\beta_{\tilde{u}_s}$. Finally, in the lower part of the outer region a small wave-induced pressure gradient develops to balance the small wave-induced stress gradient. This leads to an additional shift in the surface pressure minimum away from the wave crest, namely β_o.

There are interesting differences between the sheltering for fast and slow waves. When the waves are slow the surface stress is positive, $\tilde{\tau}_s > 0$, and the stress at the top of the inner region is negative, $\tilde{\tau}_i < 0$. Hence the change in stress, $\tilde{\tau}_s - \tilde{\tau}_i$, is large, so there is a strong sheltering effect and substantial values of β_{z_s}. In contrast, when the waves are fast the wind near the surface is against the direction of wave propagation so the wave-induced surface stress is negative, $\tilde{\tau}_s < 0$. The stress at the top of the inner region remains negative, $\tilde{\tau}_i < 0$. The net change in stress across the inner region is therefore much smaller and the sheltering is weaker. The orbital velocity at the wave surface tends to displace streamlines upwind of the wave crests and the magnitude of the effect increases with the strength of the orbital velocites, and so also with increasing wave speed, c. Finally, the contribution to β from the pressure variations at the bottom of the outer region, where the mixing-length model is being damped to zero, is positive for slow waves and negative for fast waves.

4. Growth and decay of the waves

The wave-induced pressure and stress do work at rate S_w at the wave surface, which then leads to an energy flux into or out of the wave motions, thence leading to wave growth or decay. Following Davis (1972) and Belcher & Hunt (1993), this evolution can be studied by forming an equation for the rate that the stress does work at the surface. If only the leading-order quadratic terms are retained then three sources of working contribute to S_w, namely

$$S_w = \langle \tilde{\sigma}_{ij}\tilde{u}_i n_j \rangle = \langle -c\{-\tilde{p}_s + \tilde{\tau}_{33s}\}\mathrm{d}z_s/\mathrm{d}\xi \rangle + \langle \tilde{\tau}_s \tilde{u}_s \rangle, \tag{4.1}$$

where $\langle\ \rangle$ denotes average over a wavelength, $\tilde{\sigma}_{ij}$ is the wave-induced stress tensor, and $n_j = (-\mathrm{d}z_s/\mathrm{d}\xi, 1)$ is the normal to the surface (to the leading-order approximation). The kinematic boundary condition $\tilde{w}_s = \mathrm{D}z_s/\mathrm{D}t = -c\mathrm{d}z_s/\mathrm{d}x$ was used in evaluating the first term on the right of (4.1). The contribution from the

normal turbulent stress term is small, $-c\langle\tilde{\tau}_{33s}\mathrm{d}z_s/\mathrm{d}\xi\rangle$ (Belcher & Hunt 1993; Mastenbroek 1996). Hence only two terms need to be evaluated.

The first term, $c\langle\tilde{p}_s\mathrm{d}z_s/\mathrm{d}\xi\rangle$, can be evaluated using the solution for the asymmetric surface pressure (3.19) to yield

$$c\langle\tilde{p}_s\mathrm{d}z_s/\mathrm{d}\xi\rangle = \frac{1}{2}(ak)^2u_*^2c\,\beta, \tag{4.2}$$

where β is given by (3.22). The second term in (4.1), $\langle\tilde{\tau}_s\tilde{u}_s\rangle$, can be evaluated once the horizontal motions at the surface are specified. For deep water gravity waves when $\tilde{u}_s = \mathrm{Re}\{akce^{\mathrm{i}k\xi}\}$ this term gives

$$\langle\tilde{\tau}_s\tilde{u}_s\rangle = \frac{1}{2}(ak)^2u_*^2c\,\gamma, \tag{4.3}$$

where γ is given in (3.23).

The wavelength-averaged energy in waves on deep water is $\tilde{E} = \frac{1}{2}(\rho_w/\rho_a)ga^2$ (with the current normalisation that the density of air is one) so that

$$\frac{S_w}{\tilde{E}} = \frac{\rho_a}{\rho_w}\left(\frac{u_*}{c}\right)^2\sigma(\beta+\gamma), \tag{4.4}$$

where $\sigma = ck$ is the radian wave frequency. For a homogeneous wave field and in the absence of other processes affecting development of the waves $\partial\tilde{E}/\partial t = S_w$, so that the wave energy grows or decays exponentially in time, with an e-folding time given by the reciprocal of the right hand side of (4.4).

4.1. *The growth rate coefficient* $\beta+\gamma$

The factor, denoted here $(\beta+\gamma)$, has been intensely debated in the literature. Figure 5 shows that the present solutions agree well with Mastenbroek's (1996) fully nonlinear computations, with full second-order closure for the stress, for both fast and slow waves. The theory shows both the same variation with c/u_* and also the same variation with the relative roughness kz_0. Agreement between the computations and the theory is particularly satisfying because Belcher & Hunt (1998) have argued that the damped mixing-length model used here captures the essence of the physics parameterised in a full second-order closure. The results in figure 5 support this claim. Separate evaluation of the contributions to the growth-rate coefficient shows that it is the contribution from β_{z_s}, i.e. the contribution from sheltering, that dominates for slow waves (in agreement with Belcher & Hunt 1993). In the slow-wave regime the results computed by Mastenbroek are larger than the theoretical values as c/u_* approaches its maximum value for slow waves. At these larger values of c/u_* the inner region becomes too thick for the present approximations to apply and also the critical-layer mechanism might be contributing to wave growth at these more intermediate wave speeds. The present work also shows that it is the contribution from γ_{z_s}, i.e. working of the wave-induced shear stress at the surface, that dominates for fast waves (the sheltering term is small for fast waves as explained in §3.5). The fast-wave theory agrees well with the computations when $kz_0 = 10^{-3}$ and $20 < c/u_* < 25$.

Figure 5 also shows comparisons of values of the growth-rate coefficient from the theory with values from laboratory and open-ocean experiments collated by Plant (1984). The data lie in the slow- and intermediate-wave regimes. As has been reported by others (e.g. Mastenbroek et al. 1996; Belcher & Hunt 1998) the theoretical values are smaller than the measurements. We can offer no new explanation of this, except to point out that the values measured by Shemdin & Hsu (1967) do lie close to the theory. This is significant because Shemdin & Hsu measured growth of wind-ruffled paddle-generated waves – a configuration that is close to the configuration modelled in the present theory. In contrast the remaining measurements in figure 5 inferred the growth rate of purely wind-generated waves, which are strongly influenced by nonlinear wave–wave interactions and wave breaking (e.g. Phillips 1977 §4.6). In addition the values of wave growth from Snyder et al. (1981) (the open squares in figure 5) were obtained from measurements of the momentum flux to the waves, and so these data

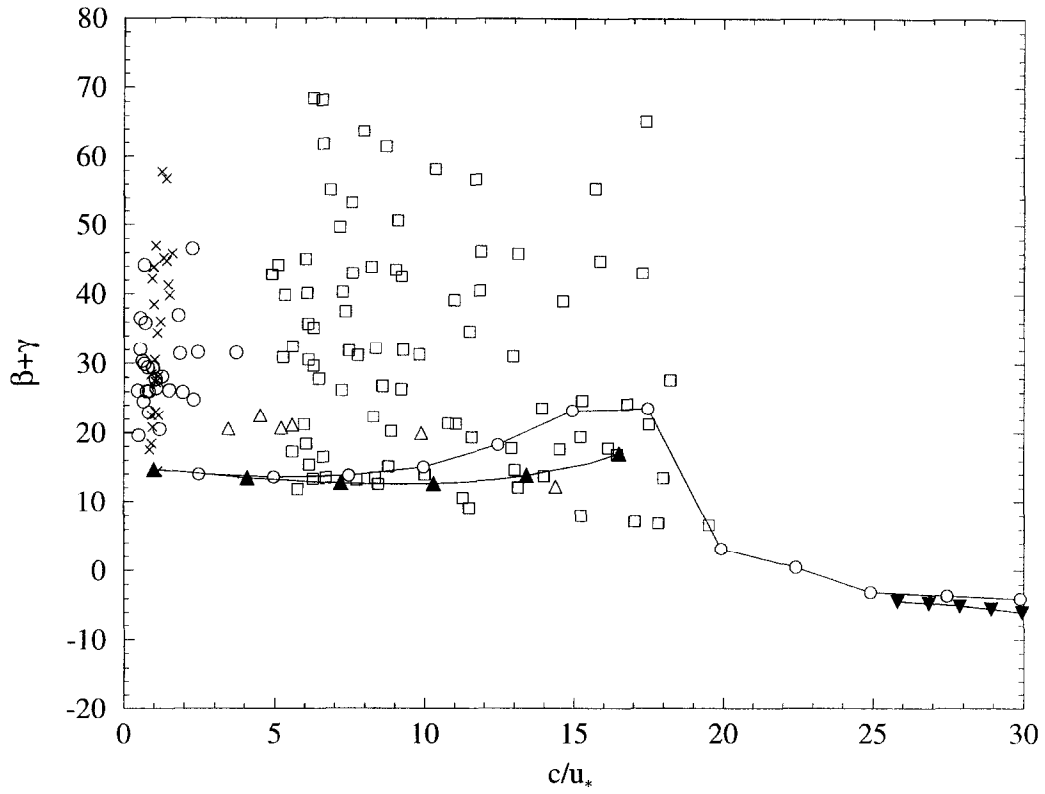

FIGURE 5. Values of the wave growth rate coefficient from the theory when $kz_0 = 10^{-4}$ (*filled triangles*) and comparisons with values computed numerically by Mastenbroek (1996) (*joined open circles*) and data collated by Plant (1982) (*other symbols*)

need to be treated with some caution. Some previous studies (e.g. Miles 1993) have reported better agreement with the data, but such claims have been made based on models that parameterise the shear stress with a mixing-length model throughout the inner and outer regions. As argued in §2.2, the mixing-length model is appropriate only in the inner region. Belcher & Hunt (1993) and others have shown that using the mixing-length model in the outer region leads to spuriously large values of the growth rate.

4.2. *A nonlinear correction to the wave growth*

The expression obtained here for the e-folding time of the waves scales on u_*^2, the surface stress in the basic-state wind profile. The present analysis shows that this basic-state wind stress controls the strength of the non-separated sheltering. It is important to recognise that this u_*^2 is not the total stress that would be measured above a wave: the total stress measured above a wind–wave system, τ_{tot}, is obtained by integrating the wave-induced stress tensor along a streamline η = constant, and is thus found to have two components

$$\tau_{tot}(\eta) = \tau_t(\eta) + \tau_w(\eta), \tag{4.5}$$

where $\tau_t = \langle \tau_B + \tilde{\tau} \rangle$ is the averaged turbulent stress and $\tau_w(\eta) = -\langle \tilde{u}\tilde{w} \rangle$ is the *wave-induced stress* (e.g. Townsend 1972).

Wave growth by non-separated sheltering

At the surface $\tau_w(z_0) = \tau_f = \langle \tilde{p}_s \mathrm{d}z_s/\mathrm{d}\xi \rangle$, where τ_f is the *form drag* (Phillips 1977), which can be evaluated from (3.19) and (3.22) to give

$$\tau_f = \frac{1}{2}(ak)^2 \beta u_*^2. \tag{4.6}$$

Furthermore, the solutions for $\tilde{u}$ and $\tilde{w}$ in the outer region show that τ_w is zero above the inner region. Hence the wave-induced stress decays from its surface value to zero above the inner region.

When averaged over a wavelength the streamwise momentum equation (the nonlinear counterpart of (2.4)) shows that the total stress is constant with height (Townsend 1972). Hence, since τ_w decreases with height, to maintain τ_{tot} constant with height, τ_t must increase with height and be larger in the outer region than in the inner region. In practice the inner region is so thin (figure 2) that measurements of the stress are likely to be taken in the outer region, where τ_t is larger than its surface value.

The analysis presented in §3 shows clearly that it is the turbulent stress that generates the non-separated sheltering and thence forces wave growth. Hence, following the spirit of the argument of Makin, Kudryavtsev & Mastenbroek (1995), in their calculation of the drag of the sea surface, we can suggest a nonlinear correction to the wind-input term S_w, namely that the factor of u_*^2 in (4.4) and (4.6) is replaced by the surface value of the averaged turbulent stress, $\tau_t(z_0)$ which is given by

$$\tau_t(z_0) = \tau_{tot} - \tau_w(z_0) = \tau_{tot} - \frac{1}{2}(ak)^2 \beta u_*^2 \to \tau_{tot} - \frac{1}{2}(ak)^2 \beta \tau_t \tag{4.7}$$

so that

$$\tau_t(z_0)/\tau_{tot} = \frac{1}{1 + \frac{1}{2}(ak)^2\beta} \quad \text{and} \quad \tau_f/\tau_{tot} = \frac{\frac{1}{2}\beta(ak)^2}{1 + \frac{1}{2}(ak)^2\beta}. \tag{4.8}$$

The wind input of energy then becomes

$$\frac{S_w}{\tilde{E}} = \frac{\rho_a}{\rho_w} \frac{\beta + \gamma}{1 + \frac{1}{2}(ak)^2\beta} \frac{\tau_{tot}}{c^2} \sigma, \tag{4.9}$$

where τ_{tot} is the turbulent stress that would be measured in the outer region. Van Duin (1996*a*) obtained a similar equation based on a rigorous, weakly nonlinear, analysis of the air flow over slow waves. Here we have shown that the nonlinear correction arises for both slow and fast waves, and it arises because the wave absorbs momentum from the air flow, i.e. there is a wave-induced stress, which depletes the turbulent stress near the surface, thereby leaving a reduced level of turbulent stress near the surface to force the non-separated sheltering.

It is clear from (4.9) that nonlinear effects reduce the growth rate of steeper waves, which is consistent with the numerical calculations of Gent & Taylor (1976) and Mastenbroek (1996). Figure 6 shows the variation of a related quantity, namely the form drag, with wave slope for a rigid wavy wall, with $c/u_* = 0$. It is clear from the figure that the nonlinear theory (4.8) lies much closer to the computations than the linear theory (4.6), particularly when $ak > 0.2$. The theoretical curves are truncated when $ak = 0.3$ because the air flow is expected to separate for higher slopes. The strength of the nonlinear effects depend on the factor $\frac{1}{2}(ak)^2\beta$, and thus depends on c/u_*. For slow waves, with small values of c/u_*, $\beta \approx 20$ so that nonlinear effects become appreciable when $ak \approx 1/(\beta)^{\frac{1}{2}} \approx \frac{1}{5}$, in agreement with the plots in figure 6. Mitsuyasu & Honda (1982) measured the growth rate of paddle-generated water waves and found that in their range of $0.03 < ak < 0.2$ (assuming that their H equals $2a$) the growth rate was insensitive to the wave slope, again in rough agreement with figure 6. For fast waves, with large values of c/u_*, $\beta \approx -1$ and much larger slopes are required for the nonlinear effects to be significant. We expect ocean waves that lie in the fast-wave regime, for example swell, to have low slopes and hence we conclude that the nonlinear effects are likely to be negligible for fast waves. Finally, we do not expect the present form of the nonlinear correction to be valid when the waves break, because

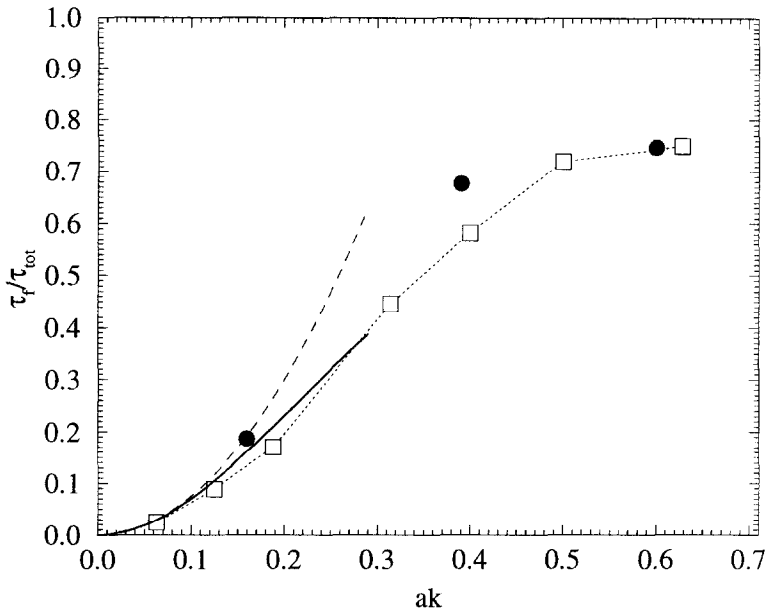

FIGURE 6. Variation of the form drag with wave slope for $c/u_* = 0$. Dashed line: linear theory; solid line: nonlinear theory; open squares: nonlinear numerical calculations with full second order closure from Belcher et al. (1993); filled circles: measurements of Zilker & Hanratty (1979) over solid wavy wall.

then the air flow separates and the streamlines no longer follow the wave surface as they are assumed to do in the present analysis. Nevertheless, the present formula should be valid up until breaking.

5. Conclusions

We have developed a heurstic analysis of the air flow over waves in the limits of slow waves, when $c/u_* < 15$, and of fast waves, when $c/u_* > 25$. Previously published formal asymptotic solutions (Belcher & Hunt 1993; Cohen & Belcher 1999) have shown that *non-separated sheltering* is the primary mechanism responsible for the growth and decay of these waves. The critical-layer mechanism is, at most, of secondary importance in these parameter regimes.

The heuristic analysis developed here aimed to understand more deeply the physical processes behind non-separated sheltering. The analysis has shown how the streamline displacement at the top of the inner region is controlled by three processes: displacement over the undulating wave surface, a Bernoulli displacement associated with pressure variations, and a small, but important, asymmetric displacement due to the turbulent shear stress. This asymmetric displacement of streamlines leads to deceleration of the wind in the lee of the wave, i.e. to a non-separated sheltering. Above the inner region, in the outer region, the streamline displacement remains in phase with the streamline at the top of the inner region: no further asymmetry is produced because the wave-induced shear-stress gradient there is too weak. A pressure perturbation then develops in the outer region that has its minimum displaced downwind of the wave crest. This pressure perturbation together with

the surface stress perturbation does work at the wave surface and leads to growth of slow waves and decay of fast waves.

The present approach shows clearly how the change in value of the shear stress across the inner region controls the strength of the non-separated sheltering. This observation suggested a nonlinear correction wherein the surface value of the turbulent stress is used in the equation for the energy flux. This surface value of the turbulent stress is smaller than the value aloft in the outer region because some of the momentum in the inner region is absorbed as wave-induced stress, which leads to a correction to the energy flux that increases as the square of the wave slope. The strength of the nonlinear correction also scales on β, the part of the growth rate coefficient that is determined by the surface pressure. Since β is larger for slow waves than for fast waves we conclude that slow waves are more likely to be affected by this nonlinear process than fast waves.

Finally, in the intermediate range of $15 < c/u_* < 25$ the critical-layer mechanism may well be important in addition to non-separated sheltering, although we note the comment of Mastenbroek (1996) that he found no evidence of a critical-layer mechanism contributing to wave growth in his numerical calculations. To date there has been no local analysis of both non-separated sheltering and the critical-layer mechanisms. Miles (1996) develops an integral analysis, but this mathematical method might exaggerate the critical-layer effects. There is hope that the present formulation, wherein the streamline displacement is analysed, can shed light onto this mathematically-difficult intermediate regime, because Belcher *et al.* (1998) have shown how an inviscid critical layer can be analysed in this framework.

Acknowledgements

It is a pleasure to thank Julian Hunt for useful discussions and suggestions during the course of this work. Funding for this work was provided partly by the EC under the ASPEN project, contract ENV4-CT97-0460 and partly by DERA under contract LSC/2034/222.

References

[1] Belcher, S. E. & Hunt, J. C. R. 1993 Turbulent shear flow over slowly moving waves. *J. Fluid Mech.* **251**, 109–148.
[2] Belcher, S. E. & Hunt, J. C. R. 1998 Turbulent flow over hills and waves. *Ann. Rev. Fluid Mech.* **30**, 507–538.
[3] Belcher, S. E., Hunt, J. C. R. & Cohen, J. E. 1998 Turbulent shear flow over growing waves *To appear in Proc. I.M.A. conference on wind–wave interactions.* Eds. S. Sajjadi, N.H. Thomas, J.C.R. Hunt. Oxford.
[4] Belcher, S. E., Newley, T. M. J. & Hunt, J. C. R. 1993 The drag on an undulating surface induced by the flow of a turbulent boundary layer. *J. Fluid Mech.* **249**, 557–596.
[5] Britter, R. E., Hunt, J. C. R. & Richards, K. J. 1981 Air flow over a 2-d hill: studies of velocity speed up, roughness effects and turbulence. *Q. J. R. Met. Soc.* **107**, 91–110.
[6] Cohen, J. E. & Belcher, S. E. 1999 Turbulent shear flow and fast moving waves. *J. Fluid Mech. In press*
[7] Davies, R. E. 1972 On prediction of turbulent flow over a wavy boundary. *J. Fluid Mech.* **52**, 287–306.
[8] Duin, C. A. van 1996a An asymptotic theory for the generation of nonlinear surface gravity waves by turbulent air flow. *J. Fluid Mech.* **320**, 287–304.
[9] Duin, C. A. van 1996b Rapid-distortion turbulence models in the theory of surface-wave generation. *J. Fluid Mech.* **329**, 147–153.
[10] Gent, P. R. & Taylor, P. A. 1976 A numerical model of the air flow above water waves. *J. Fluid Mech.* **77**, 105–128.
[11] Hunt, J. C. R., Leibovich, S. & Richards, K. J. 1988 Turbulent shear flow over low hills. *Q. J. R. Met. Soc.* **114**, 1435–1471.
[12] Hunt, J. C. R. & Richards, K. J. 1984 Stratified airflow over one or two hills. *Boundary-Layer Met.* **30**, 223–259.
[13] Jeffreys, H. 1925 On the formation of water waves by wind. *Proc. R. Soc. Lond.* **A 107**, 189–206.
[14] Makin, V. K., Kudryavstev, V. N., & Mastenbroek, C. 1995 Drag of the sea surface. *Boundary Layer Meteorol.* **73**, 159–182.
[15] Mastenbroek, C. 1996 *Wind–wave interaction*, PhD thesis, Delft Technical University.
[16] Mastenbroek, C., Makin, V. K., Garat, M. H. & Giovanangeli, J. P. 1996 Experimental evidence of the rapid distortion of the turbulence in the air flow over water waves. *J. Fluid Mech.* **318**, 273–302.
[17] Miles, J. W. 1957 On the generation of surface waves by shear flows. *J. Fluid Mech.* **3**, 185–204.
[18] Miles, J. W. 1993 Surface-wave generation revisited. *J. Fluid Mech.* **256**, 427–441.
[19] Miles, J. W. 1996 Surface-wave generation: a viscoelastic model. *J. Fluid Mech.* **322**, 131–145.
[20] Phillips, O. M. 1977 *The Dynamics of the Upper Ocean.* C. U. P.
[21] Plant, W. J. 1984 A relationship between wind shear stress and wave slope. *J. Geophys. Res.* **87**, C3, 1961–1967.

[22] SHEMDIN, O. H. & HSU, E. Y. 1967 The dynamics of wind in the vicinity of progressive water waves. *J. Fluid Mech.* **30**, 403–416.
[23] SNYDER, R. L., DOBSON, F. W., ELLIOT, J. A., LONG, R. B. 1981 Array measurements of atmospheric pressure fluctuations above gravity waves. *J. Fluid Mech.* **102**, 1–59.
[24] TOWNSEND, A. A. 1972 Flow in a deep turbulent boundary layer disturbed by water waves. *J. Fluid Mech.* **55**, 719–735.
[25] ZOU, Q. P. 1998 A viscoelastic model for turbulent flow over undulating topography. *J. Fluid Mech.*, **355**, 81–112.
[26] ZILKER, D. P. & HANRATTY, T. J. 1979 Influence of a solid way boundary on turbulent flow. Part 2 separated flows. *J. Fluid Mech.*, **90**, 257–271.